

(S)-4,5-Dihydro-2-(2-hydroxy-4-hydroxyphenyl)-4-methyl-4-thiazolecarboxylic Acid Polyethers: A Solution to Nephrotoxicity

Raymond J. Bergeron,* Jan Wiegand, James S. McManis, John R. T. Vinson, Hua Yao, Neelam Bharti, and James R. Rocca†

Department of Medicinal Chemistry and the Advanced Magnetic Resonance Imaging and Spectroscopy Facility, University of Florida, Gainesville, Florida 32610-0485

Received September 9, 2005

Previous studies revealed that within a family of ligands the more lipophilic chelators have better iron-clearing efficiency. The larger the $\log P_{\text{app}}$ value of the compound, the better the iron-clearing efficiency. What is also clear from the data is that although the relative effects of $\log P_{\text{app}}$ changes are essentially the same through different families, there are differences in absolute value between families. However, there also exists a second, albeit somewhat more disturbing, relationship. In all sets of ligands, the most lipophilic chelator is always the most toxic. The current study focuses on designing ligands that balance the lipophilicity/toxicity problem while iron-clearing efficiency is maintained. Earlier studies with (S)-4,5-dihydro-2-(2-hydroxy-4-methoxyphenyl)-4-methyl-4-thiazolecarboxylic acid [(S)-4'-(CH₃O)-DADFT, **6**] indicated that this methyl ether was a ligand with excellent iron-clearing efficiency in both rodents and primates; however, it was too toxic. On the basis of this finding, a less lipophilic, more water-soluble ligand than **6** was assembled, (S)-4,5-dihydro-2-[2-hydroxy-4-(3,6,9-trioxadecyloxy)phenyl]-4-methyl-4-thiazolecarboxylic acid [(S)-4'-(HO)-DADFT-PE, **11**], a polyether analogue, along with its ethyl and isopropyl esters. The parent polyether and its isopropyl and ethyl esters were all shown to be highly efficient iron chelators in both rodents and primates. A comparison of **11** in rodents with the desferrithiocin analogue (S)-4,5-dihydro-2-(2,4-dihydroxyphenyl)-4-methyl-4-thiazolecarboxylic acid [(S)-4'-(HO)-DADFT, **1**] revealed the polyether to be more tolerable, achieving higher concentrations in the liver and significantly lower concentrations in the kidney. The lower renal drug levels are in keeping with the profound difference in the architectural changes seen in the kidney of rodents given **1** versus those treated with **11**.

Introduction

Humans have evolved a highly efficient iron management system in which we absorb and excrete only about 1 mg of the metal daily; there is no mechanism for the excretion of excess iron.¹ Two systemic “iron processing” proteins are involved, one for transport, transferrin, and the other for storage, ferritin. Introduction of excess iron into this closed system, whether derived from transfused red blood cells^{2–4} or from increased absorption of dietary iron,^{5,6} leads to a build up of the metal in the liver, heart, pancreas, and elsewhere. Such accumulation eventually produces (i) liver disease that may progress to cirrhosis,^{7–9} (ii) diabetes related both to iron-induced decreases in pancreatic β -cell secretion^{10,11} and increases in hepatic insulin resistance, and (iii) heart disease, still the leading cause of death in thalassemia major^{12–14} and related forms of transfusional iron overload. The precise pathways of iron deposition and its regulation are incompletely understood, but the available evidence suggests that these differ in the liver, physiologically a major systemic iron depot, and in the pancreas and heart, which normally do not serve as iron storage sites. Recent evidence suggests that L-type Ca²⁺ channels constitute a major pathway for iron entry into cardiomyocytes from plasma nontransferrin bound iron (NTBI).¹⁵ Similar L-type Ca²⁺ channels are present in pancreatic β -cells and cells of the anterior pituitary but are not found in hepatocytes or Kupffer cells.

There are a number of disease states in which the body iron stores and plasma NTBI levels are sufficiently high to cause significant oxidative tissue damage. The Fenton reaction,^{16–19}

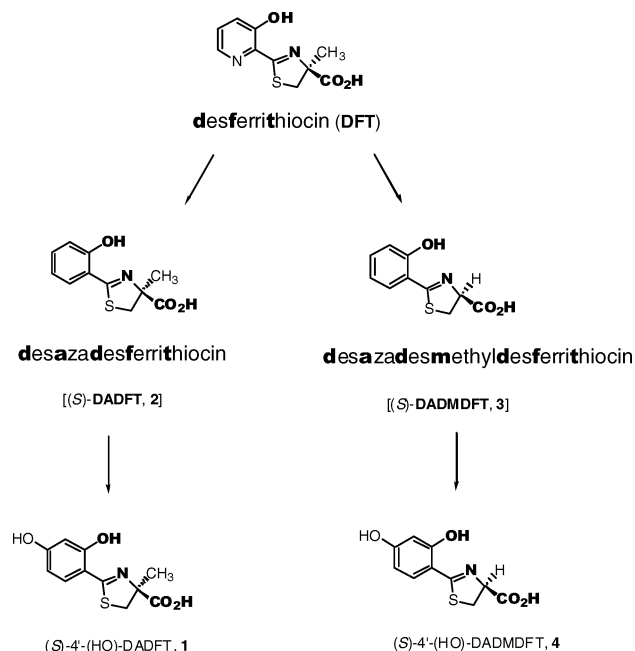
reaction of Fe(II) with endogenous hydrogen peroxide to produce the hydroxyl radical, a very reactive species, and the hydroxide anion, is repudiated to be a major source of the tissue damage associated with excess iron. The hydroxyl radical reacts very quickly with a variety of cellular constituents and can initiate free radicals and radical-mediated chain processes that damage DNA and membranes, as well as produce carcinogens. The Fe(III) liberated can be reduced back to Fe(II) via a variety of biological reductants, a problematic cycle. Some iron chelators inhibit the Fenton reaction [e.g., desferrioxamine B (DFO¹⁸)]; paradoxically, others stimulate it [e.g., 1,2-dimethyl-3-hydroxypyridin-4-one (deferiprone, L1)].²⁰ Although the precise nature of iron-mediated damage is complex¹⁸ and remains somewhat elusive, the solution is clear: identify chelators that will sequester this transition metal and render it excretable without promoting Fenton chemistry.

In the majority of patients with thalassemia major or other transfusion-dependent refractory anemias, treatment with a chelating agent capable of sequestering iron and permitting its excretion from the body is the only therapeutic approach available. The iron-chelating agents now in use or under clinical evaluation are DFO, L1, the Novartis triazole 4-[3,5-bis(2-hydroxyphenyl)-1,2,4-triazol-1-yl]benzoic acid (ICL670A), and our own desferrithiocin [(S)-4,5-dihydro-2-(3-hydroxy-2-pyridinyl)-4-methyl-4-thiazolecarboxylic acid, DFT] analogue (S)-4,5-dihydro-2-(2,4-dihydroxyphenyl)-4-methyl-4-thiazolecarboxylic acid [(S)-4'-(HO)-DADFT, **1**] (Chart 1).

DFO, a naturally occurring hexadentate trihydroxamic acid, although used clinically, is poorly absorbed from the gastrointestinal (GI) tract and rapidly eliminated from the circulation, necessitating prolonged (8–12 h daily) parenteral [subcutaneous (sc) or intravenous (iv)] infusion.^{21–24} Not surprisingly,

* Corresponding Author. Phone (352) 846-1956. Fax (352) 392-8406. E-mail: rayb@ufl.edu.

† Advanced Magnetic Resonance Imaging and Spectroscopy Facility.

Chart 1. Initial Structural Alterations in the Tridentate Chelator Desferrithiocin (DFT)^a

^a Abbreviations used throughout the text were derived from the names of **2** and **3**, as shown by the boldface letters. The ligating sites are also in bold text.

patients have difficulty with this demanding regimen, and considerable effort has been devoted to finding suitable alternatives.

The orally active bidentate chelator L1 is licensed in Europe and some other countries as second-line therapy to DFO. Unfortunately, although it is orally active, it is less efficient than DFO at removing iron.^{25–28} Whereas the orally active tridentate chelator ICL670A has now been approved by the FDA, it did not demonstrate noninferiority to DFO. Furthermore, it apparently has a somewhat narrow therapeutic window, owing to potential nephrotoxicity.^{29–31}

Ligand **1** is an orally active tridentate DFT analogue now in phase I/II trials in patients. Although the preclinical toxicity profile of **1** was relatively benign, i.e., no geno- or reproductive toxicity and only mild nephrotoxicity at high doses, the clinical results remain to be elucidated.

All of these agents predominantly chelate iron derived from systemic storage sites, either from iron released by macrophages after catabolism of senescent red blood cells, from iron in hepatic pools, or from both. Almost daily administration of near maximal tolerated doses of the first three agents is required to keep pace with rates of transfusion iron loading in patients with thalassemia major and other refractory anemias. As a consequence of the major systemic source of chelated iron, each of these agents is maximally effective when given to prevent the accumulation of a toxic iron burden and to maintain a low level of body iron stores. In patients who accumulate substantial body iron burdens, the metal builds up in vulnerable organs. Prolonged, intensive therapy is then needed to arrest progression of the complications of iron overload or, in the case of heart disease, to reverse cardiac dysfunction. For example, in patients with thalassemia major who present with cardiac failure, daily 24-h infusions of DFO for periods of years are required to reverse the iron-induced heart disease.³²

We believe that there is a pressing need for the continued development of new iron-chelating agents that are more effective and/or that can selectively remove iron from organs especially

vulnerable to iron-induced toxicity. Ligands that are more effective would be able to more rapidly reduce dangerous body iron burdens to safer levels and forestall the development or progression of complications. Iron-chelating agents that could selectively enter cardiac, pancreatic, or hepatic cells could help immediately reduce toxic iron pools and provide prompt protection against the progression of injury. Especially with respect to heart disease, still the cause of death in 70% or more of patients with thalassemia major, the availability of such agents could be life-saving.

However, the underlying problem of nephrotoxicity is the subset of the current work, in particular as this issue relates to DFT analogues. This study focuses on the design, synthesis, and testing of DFT analogues that are very efficient iron chelators with minimal nephrotoxicity.

Results and Discussion

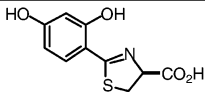
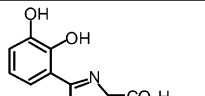
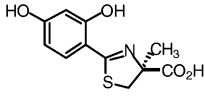
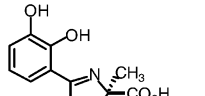
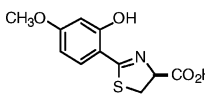
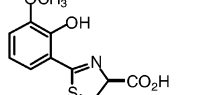
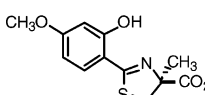
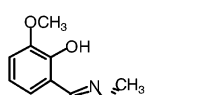
Design Concept. DFT is a tridentate siderophore³³ that forms a stable 2:1 complex with Fe(III); the cumulative formation constant is $4 \times 10^{29} \text{ M}^{-1}$.^{34,35} It performed well when given orally (po) in both the bile duct-cannulated rodent model (ICE, 5.5%)³⁶ and in the iron-overloaded *Cebus apella* primate (ICE, 16%).^{37,38} Unfortunately, DFT is severely nephrotoxic.³⁸ Nevertheless, the outstanding oral activity spurred a structure–activity study to identify an orally active and safe DFT analogue. Our initial goal was to define the minimal structural platform compatible with iron clearance upon po administration.

Our approach first entailed simplifying the platform. Removal of the pyridine nitrogen of DFT gave (S)-4,5-dihydro-2-(2-hydroxyphenyl)-4-methyl-4-thiazolecarboxylic acid [(S)-DADFT, **2**], the parent ligand of the desaza (DA) series. Substitution of the 4-methyl with hydrogen, as well, led to (S)-4,5-dihydro-2-(2-hydroxyphenyl)-4-thiazolecarboxylic acid [(S)-DADMDFT, **3**], the very simple desazadesmethyl (DADM) system (Chart 1). Although chelators **2** and **3** were still very effective iron chelators, they were plagued with GI toxicity rather than nephrotoxicity.³⁹ Further structure–activity studies were aimed at ameliorating these toxicity problems. By altering the lipophilicity (i.e., partition properties, $\log P_{\text{app}}$) and/or the redox potential of the aromatic ring, the drug's toxicity profile, organ distribution properties, and potential metabolic disposition could change.

It was ultimately determined that hydroxylation, as in the systems (S)-4'-(HO)-DADFT (**1**) or (S)-2-(2,4-dihydroxyphenyl)-4,5-dihydro-4-thiazolecarboxylic acid [(S)-4'-(HO)-DADMDFT, **4**] (Chart 1), was compatible with iron clearance in the primate model and also profoundly reduced toxicity in rodents.^{39–41} Previous studies indicate that the dose-limiting toxicity of **1** in rodents was nephrotoxicity.⁴⁰ Although the origin of the nephrotoxicity is unclear, the target seems to be centered largely in the proximal tubules. The current study focuses on structural alterations of **1** that, which while not diminishing the iron-clearing efficiency of the parent drug, reduce the level of chelator achieved in the kidney. These alterations are shown to have a profound effect both on how the drug distributes to the kidneys, as well as how it impacts the proximal tubules.

Previous studies revealed that within a family of ligands the more lipophilic compounds have better iron-clearing efficiency. For example, in an earlier study⁴² we evaluated the impact of altering the lipophilicity, $\log P_{\text{app}}$, of both (S)-4'-(HO)-DADFTs (compounds **1**, **4–6**, Table 1) and (S)-2-(2,3-dihydroxyphenyl)-4,5-dihydro-4-thiazolecarboxylic acids [(S)-3'-(HO)-DADFTs], (compounds **7–10**, Table 1). We found that the larger the log

Table 1. Iron-Clearing Activity of Desferrithiocin Analogues When Administered Orally to Iron-Loaded *C. apella* Primates and the Partition Coefficients of the Compounds^a

| 4'-Substituted Compounds | | | 3'-Substituted Compounds | | |
|---|---|--|--|---|--|
| Desferrithiocin Analogue (compd. no.) | Iron-Clearing Efficiency (%) ^b | log <i>P</i> _{app} ^c | Desferrithiocin Analogue (compd. no.) | Iron-Clearing Efficiency (%) ^b | log <i>P</i> _{app} ^c |
|  (<i>S</i>)-4'-(HO)-DADMDFT (4) | 4.2 ± 1.4 ^d [70/30] | -1.33 |  (<i>S</i>)-3'-(HO)-DADMDFT (7) | 5.8 ± 3.4 ^e [91/9] | -1.67 |
|  (<i>S</i>)-4'-(HO)-DADFT (1) | 13.4 ± 5.8 ^f [86/14] | -1.05 |  (<i>S</i>)-3'-(HO)-DADFT (8) | 23.1 ± 5.9 ^g [83/17] | -1.17 |
|  (<i>S</i>)-4'-(CH ₃ O)-DADMDFT (5) | 16.2 ± 3.2 ^f [81/19] | -0.89 |  (<i>S</i>)-3'-(CH ₃ O)-DADMDFT (9) | 15.5 ± 7.3 ^g [87/13] | -1.52 |
|  (<i>S</i>)-4'-(CH ₃ O)-DADFT (6) | 24.4 ± 10.8 ^f [91/9] | -0.70 |  (<i>S</i>)-3'-(CH ₃ O)-DADFT (10) | 22.5 ± 7.1 ^g [91/9] | -1.12 |

^a Adapted from ref 42. ^b In the monkeys, *n* = 4 (**1**, **4**, **5**, **8**), 7 (**6**), 5 (**10**), 6 (**9**), or 8 (**7**). The primates were given a single 150 μmol/kg dose of the chelators. The efficiency of each compound was calculated by averaging the iron output for 4 days before the administration of the drug, subtracting these numbers from the 2-day iron clearance after the administration of the drug, and then dividing by the theoretical output; the result is expressed as a percent. The relative percentages of the iron excreted in the stool and urine are in brackets. ^c Data are expressed as the log of the fraction in the octanol layer (log *P*_{app}); measurements were done in Tris buffer, pH 7.4, using a "shake flask" direct method. The values obtained for compounds **1** and **4–6** are from ref 41. ^d Data are from ref 39. ^e Data are from ref 40. ^f Data are from ref 41. ^g Data are from ref 42.

*P*_{app} value of the compound, the greater the iron-clearing efficiency. What is also clear from the data is that although the relative effects of log *P*_{app} changes are essentially the same for (*S*)-4'-(HO)-DADFTs and (*S*)-3'-(HO)-DADFTs, there are differences in absolute value between families.

However, there also exists a second, albeit somewhat more disturbing, relationship. The greater the lipophilicity of a chelator, the more toxic it is. The ligands in Table 2 can be separated into three families: the DADMDFTs (**3** and **4**), the DADFTs (**1**, **2**, **6** and **11**), and the Me₂-DADMDFTs (**12** and **13**). In each family, as the lipophilicity decreases, i.e., the log *P*_{app} becomes more negative, the toxicity also decreases. Reduction in the lipophilicity of (*S*)-DADMDFT (**3**) was accomplished by simple 4'-hydroxylation of the aromatic ring to generate **4**. In the DADFT series, again, hydroxylation of the 4' aromatic position moving from **2** to **1** or, as will be seen below, introduction of the polyether into **2** to produce (*S*)-4'-(HO)-DADFT-PE (**11**) produced similar results: profound reductions in toxicity. Finally, hydroxylation of (*S*)-5,5-Me₂-DADMDFT (**12**) to (*S*)-5,5-Me₂-4'-(HO)-DADMDFT (**13**) is also consistent with the idea that 4'-hydroxylation and/or reduction in lipophilicity can have a significant effect on ligand toxicity within a family of chelators. The data suggested it would be possible to further operate on a ligand to optimize the lipophilicity/iron clearance/toxicity profile.

Earlier studies with (*S*)-4,5-dihydro-2-(2-hydroxy-4-methoxyphenyl)-4-methyl-4-thiazolecarboxylic acid [(*S*)-4'-(CH₃O)-DADFT (**6**)] indicated it to be a ligand with excellent iron-clearing efficiency in both rodents and primates.⁴² Thus, there is nothing implicit in the alkylation of the 4'-(HO) of **1** that

suggests a reduction in iron clearance. In fact, the data was consistent with improved iron-clearing efficiency. However, this alkylation, methylation of **1** to **6**, was found to elicit pronounced nephrotoxicity when **6** was given sc to rats at a dose of 300 μmol/kg/d for 5 d (unpublished data). Rodents treated with **1** under an identical dosing regimen did not exhibit any renal toxicity. Nevertheless, the fact that **6** was a significantly better iron chelator in rodents than the parent **1** encouraged the pursuit of a less lipophilic, more water-soluble ligand than **6**. It was felt that such a ligand was likely to be cleared from the kidneys more quickly, thus lowering the steady-state tissue concentration and therefore toxicity. The current study focuses on designing ligands that balance the lipophilicity/toxicity interaction while iron-clearing efficiency is maintained. The ligand of choice was the polyether (*S*)-4,5-dihydro-2-[2-hydroxy-4-(3,6,9-trioxadecyloxy)phenyl]-4-methyl-4-thiazolecarboxylic acid [(*S*)-4'-(HO)-DADFT-PE, **11**].

Synthetic Methods. The synthesis of (*S*)-4'-(HO)-DADFT-PE (**11**) began with the conversion of (*S*)-4'-(HO)-DADFT (**1**) to its isopropyl ester **14** in 99% yield with 2-iodopropane (1.9 equiv) and *N,N*-diisopropylethylamine (1.9 equiv, DIEA) in DMF (Scheme 1). Ester **14** was then alkylated at the 4'-hydroxyl using an equimolar amount of tri(ethylene glycol) monomethyl ether under Mitsunobu conditions [diisopropyl azodicarboxylate (1.2 equiv, DIPAD) and triphenylphosphine (1.2 equiv) in THF], providing (*S*)-4'-(HO)-DADFT-PE-*i*PrE (**15**) in 76% yield. Hydrolysis of isopropyl ester **15** with 50% NaOH (13 equiv) in methanol followed by acidification with dilute HCl furnished (*S*)-4'-(HO)-DADFT-PE (**11**) in 95% yield. Esterification of

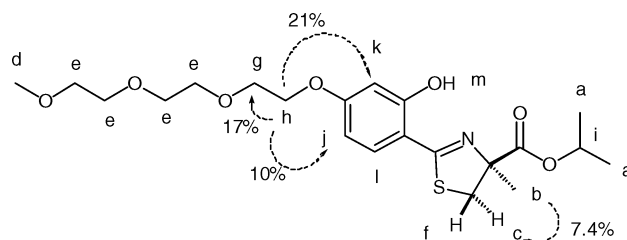
Table 2. Partition Coefficients and Tolerability of DFT Analogues^a

| Number | Structure | Log P_{app} | Tolerability |
|--------|-----------|----------------------|-------------------------|
| 3 | | -0.93 | All rats dead by day 6. |
| 4 | | -1.33 | All rats survived. |
| 2 | | -0.34 | All rats dead by day 5. |
| 1 | | -1.05 | All rats survived. |
| 6 | | -0.70 | All rats dead by day 6. |
| 11 | | -1.1 | All rats survived. |
| 12 | | -0.34 | All rats dead by day 6. |
| 13 | | -0.91 | All rats survived. |

^a All compounds were given to the rats orally by gavage at a dose of 384 $\mu\text{mol/kg/d}$ for a maximum of 10 days.

polyether acid **11** with iodoethane (1.6 equiv) by the method of **14** afforded (*S*)-4'-(HO)-DADFT-PE-EE (**16**) in 83% yield.

That substitution of resorcinol derivative **14** occurred at the 4'-hydroxyl and not the more sterically hindered 2'-hydroxyl, giving monoadduct **15**, was verified by NOE difference spectroscopy. Irradiation at δ 4.14, assigned to methylene (h) of the triether chain, significantly enhanced *two* aromatic signals— δ 6.46 (j) and 6.49 (k)—as well as the adjacent methylene of the linear chain at δ 3.86 (g) (Figure 1). Moreover, irradiation at δ 1.64, the signal corresponding to the 4-methyl



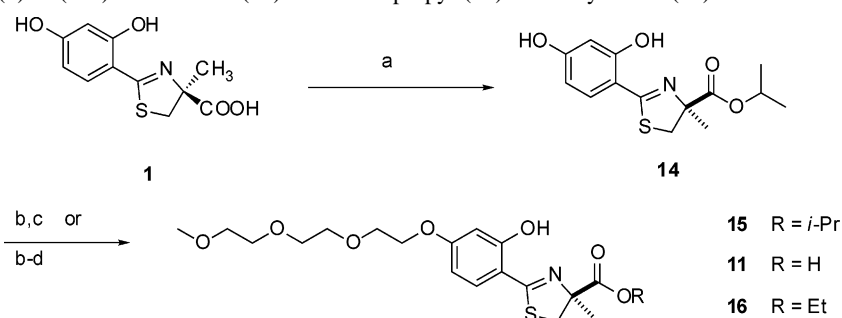
| ¹ H Assignment (15) | δ (multiplicity, integration, coupling constant in Hz) |
|---|---|
| a | 1.26 (d, 3 H, $J = 6.2$) |
| a | 1.28 (d, 3 H, $J = 6.2$) |
| b | 1.64 (s, 3 H) |
| c | 3.18 (d, 1 H, $J = 11.2$) |
| d | 3.38 (s, 3 H) |
| e | 3.54-3.57 (m, 2 H) |
| e | 3.64-3.66 (m, 2 H) |
| e | 3.67-3.69 (m, 2 H) |
| e | 3.72-3.74 (m, 2 H) |
| f | 3.83 (d, 1 H, $J = 11.2$) |
| g | 3.86 (t, 2 H, $J = 4.8$) |
| h | 4.14 (t, 2 H, $J = 4.8$) |
| i | 5.07 (septet, 1 H, $J = 6.2$) |
| j | 6.46 (dd, 1 H, $J = 8.7, 2.3$) |
| k | 6.49 (d, 1 H, $J = 2.3$) |
| l | 7.28 (d, 1 H, $J = 8.7$) |
| m | 12.6 (s, 1 H) |

Figure 1. ¹H resonances and pertinent homonuclear NOE correlations for (*S*)-4'-(HO)-DADFT-PE-*i*PrE (**15**); the percent NOE is indicated next to the dotted lines.

group (b), enhanced the upfield thiazolidine methine doublet at δ 3.18 (c); thus, these ring substituents are syn.

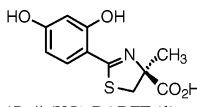
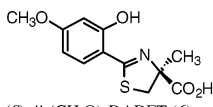
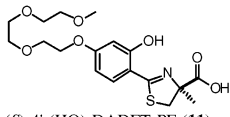
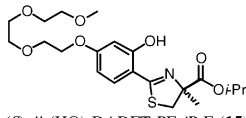
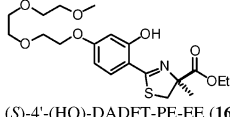
Chelator-Induced Iron Clearance in Non-Iron-Overloaded Rodents. When describing the effects of structural alterations on the DFT skeleton, the iron-clearing efficiencies of the compounds in rats are shown (Table 3), along with the relative fractions of the iron excreted in the bile and in the urine. A single 300 $\mu\text{mol/kg}$ dose of drug was administered to male Sprague–Dawley rats (400–450 g) po and/or sc. We will begin with a brief discussion of (*S*)-4'-(HO)-DADFT (**1**) and (*S*)-4'-(CH₃O)-DADFT (**6**). Ligand **1** performed poorly in rodents when given either po or sc. The iron-clearing efficiencies, $1.1 \pm 0.8\%$ and $1.1 \pm 0.6\%$, respectively, were minimal at best. When **1** was 4'-(HO) methylated to provide **6**, the iron-clearing efficiency after po administration increased substantially to $6.6 \pm 2.8\%$; 98% of the iron was in the bile and 2% was in the urine. Thus, **6** performed better than the parent drug **1** ($p < 0.02$). The polyether of **1**, (*S*)-4'-(HO)-DADFT-PE (**11**), in which a 3,6,9-trioxadecyl group was fixed to the 4'-(HO) of **1**, also performed well, with an iron-clearing efficiency of $5.5 \pm 1.9\%$ and a 90/10 distribution of iron in the bile/urine when administered po. Given sc, the efficiency increased to $8.7 \pm 2.6\%$, slightly more than po ($p < 0.05$). We also investigated the iron-clearing efficiencies of the corresponding isopropyl

Scheme 1. Synthesis of (*S*)-4'-(HO)-DADFT-PE (**11**) and Its Isopropyl (**15**) and Ethyl Ester (**16**)^a



^a Reagents: (a) *i*-PrI (1.9 equiv), DIEA (1.9 equiv), DMF, rt, 14 d, 99%; (b) CH₃[O(CH₂)₂]₃OH (1.0 equiv), DIPAD (1.2 equiv), PPh₃ (1.2 equiv), THF, 5 °C, 1 d, 76%; (c) 50% NaOH (13 equiv), CH₃OH, then 1 N HCl, rt, 1 d, 95%; (d) EtI (1.6 equiv), DIEA (1.6 equiv), DMF, rt, 50 h, 83%.

Table 3. Iron-Clearing Efficiency of DFT Analogues in Non-Iron-Overloaded Rodents^a

| Structure | Vehicle | Route | N | Efficiency (%) [bile/urine] |
|---|--------------------------------|-------|---|--------------------------------|
|  (S)-4'-(HO)-DADFT (1) | dH ₂ O ^b | po | 8 | 1.1 ± 0.8 [100/0] |
| | dH ₂ O ^b | sc | 4 | 1.1 ± 0.6 [93/7] |
|  (S)-4'-(CH ₃ O)-DADFT (6) | dH ₂ O ^b | po | 4 | 6.6 ± 2.8 [98/2] |
|  (S)-4'-(HO)-DADFT-PE (11) | dH ₂ O | po | 5 | 5.5 ± 1.9 [90/10] |
| | dH ₂ O | sc | 4 | 8.7 ± 2.6 [95/5] |
|  (S)-4'-(HO)-DADFT-PE- <i>i</i> PrE (15) | 40% Cremophor | po | 5 | 13.9 ± 3.3 [95/5] |
| | 50% EtOH | sc | 6 | 22.1 ± 7.6 [95/5] |
|  (S)-4'-(HO)-DADFT-PE-EE (16) | 50% EtOH | sc | 3 | 11.4 ± 0.8 [96/4] |

^a The rodents were given a single 300 μmol/kg dose of the chelators. The efficiency of each compound was calculated by subtracting the iron excretion of control animals from the iron excretion of the treated animals. This number was then divided by the theoretical output; the result is expressed as a percent. The relative percentages of the iron excreted in the bile and urine are in brackets. ^b The compounds were solubilized by the addition of 1 equiv of NaOH to a suspension of the free acid in distilled H₂O.

ester, (S)-4'-(HO)-DADFT-PE-*i*PrE (**15**). Although the isopropyl ester (**15**) is only a bidentate ligand, nonspecific esterase cleavage would liberate the tridentate chelator **11**. Such required cleavage of **15** to the active compound (**11**) could also increase its half-life, possibly increasing iron-clearing efficiency. When administered po, the efficiency of **15** was significantly higher than that of the polyether parent **11**, 13.9 ± 3.3% versus 5.5 ± 1.9%, ($p < 0.002$) with 95% of the iron in the bile. When administered sc, the isopropyl ester (**15**) was also significantly better than **11**, 22.1 ± 7.6% versus 8.7 ± 2.6% ($p < 0.003$) with 95% of the iron in the bile. It is important to point out that because of the poor water solubility of this compound, it was administered in 50% ethanol–water. The profound difference in iron-clearing efficiencies between **15** and any other compound given sc compelled us to be sure that **15** was not being transesterified in the aqueous ethanol. The ethyl ester, (S)-4'-(HO)-DADFT-PE-EE (**16**), would likely be cleaved by nonspecific esterases more efficiently than the isopropyl ester (**15**) to the parent ligand (**11**). When we gave rodents the ethyl ester **16** in 50% aqueous ethanol sc, the iron-clearing efficiency was 11.4 ± 0.8%, significantly lower than that of the isopropyl ester **15** ($p < 0.01$). The distribution of iron was similar, 96% of the iron being excreted in the bile.

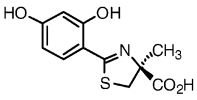
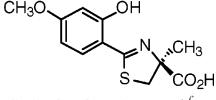
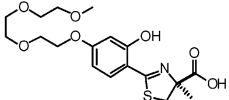
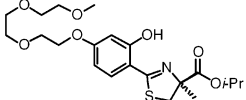
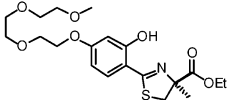
Iron Clearance in Iron-Loaded Primates. Not unexpectedly, all of the ligands performed better in the iron-loaded primates than in the non-iron-overloaded rodents (Table 4). The drugs were given po and/or sc to the monkeys at a dose of 150

μmol/kg. The efficiency of the parent drug (**1**) in the primates was 16.8 ± 7.2% when given po and 15.9 ± 2.7% when given sc. The iron distribution was largely biliary, 88/12. A similar scenario unfolded with the 4'-(CH₃O) analogue (**6**). The efficiency of the chelator given po was 24.4 ± 10.8%, with a similar iron excretion ratio of 91/9. The polyether (**11**) given po had an efficiency of 25.4 ± 7.4%. When given sc the clearance was also very impressive, 30.4 ± 7.2%. Both methods of dosing presented with largely fecal iron excretion, 96 and 99%, respectively. With the isopropyl ester (**15**) the efficiency was 19.5 ± 6.8% after po dosing, with a stool/urine iron excretion ratio of 77/23. With the polyether ethyl ester (**16**), the iron-clearing efficiency was 17.9 ± 1.0% when given sc with a feces/urine distribution of 81/19.

In addition, both **1** and **11** demonstrate excellent oral bioavailability. The po vs sc iron clearing efficiencies are nearly identical: 16.8 ± 7.2% vs 15.9 ± 2.7% for ligand **1** and 25.4 ± 7.4% vs 30.4 ± 7.2% for **11**. The efficiency of **15** po and **16** sc are within the error of the efficiency of **1** given po or sc ($p > 0.05$). Finally, although the efficiency of **11** given po is greater than that of **1** po, the increase is just shy of being significant ($p = 0.06$). However, **11** given sc is significantly more effective than **1** sc ($p < 0.02$). Nevertheless, the po and sc iron-clearing efficiencies of **11** are 500% greater than that of sc-administered DFO.³⁸

Toxicity Assessment of (S)-4'-(CH₃O)-DADFT (6**) and (S)-4'-(HO)-DADFT-PE (**11**).** Male Sprague–Dawley rats ($n = 6$

Table 4. Iron-Clearing Efficiency of DFT Analogues in Iron-Loaded Primates^a

| Structure | Vehicle | Route | N | Efficiency (%) [bile/urine] |
|---|--------------------------------|-------|---|--------------------------------|
|  (S)-4'-(HO)-DADFT (1) | dH ₂ O ^b | po | 6 | 16.8 ± 7.2 [88/12] |
| | dH ₂ O ^b | sc | 5 | 15.9 ± 2.7 [88/12] |
|  (S)-4'-(CH ₃ O)-DADFT (6) ^c | 40% Cremophor | po | 7 | 24.4 ± 10.8 [91/9] |
|  (S)-4'-(HO)-DADFT-PE (11) | dH ₂ O | po | 4 | 25.4 ± 7.4 [96/4] |
| | dH ₂ O | sc | 4 | 30.4 ± 7.2 [99/1] |
|  (S)-4'-(HO)-DADFT-PE-iPrE (15) | 40% Cremophor | po | 4 | 19.5 ± 6.8 [77/23] |
|  (S)-4'-(HO)-DADFT-PE-EE (16) | 50% EtOH | sc | 2 | 17.9 ± 1.0 [81/19] |

^a The primates were given a single 150 μmol/kg dose of the analogues. The efficiency of each compound was calculated by averaging the iron output for 4 days before the drug, subtracting these numbers from the 2-day iron clearance after the administration of the drug, and then dividing by the theoretical output; the result is expressed as a percent. The relative percentages of the iron excreted in the stool and urine are in brackets. ^b The compounds were solubilized by the addition of 1 equiv of NaOH to a suspension of the free acid in distilled H₂O. ^c Data are from ref 42.

per group) were given **6** or **11** po once daily for up to 10 d at a dose of 384 μmol/kg/d (equivalent to 100 mg/kg/d of the DFT sodium salt). In a second experiment, rats were given **11** po at a dose of 63.3 μmol/kg/d for 30 days. The latter dose was selected on the basis of primate iron clearance data, i.e., this dose represents enough ligand to clear 450 μg of Fe/kg of body weight from the primates. Dosing with **6** had to be stopped after five doses; severe nephrotoxicity, reminiscent of what was found when the ligand was given sc at 300 μmol/kg/d for 5 days (unpublished data), resulted. However, histopathological results of extensive tissues including the heart, liver, pancreas, kidney, stomach, and intestine from animals treated with **11** for 10 or 30 days were normal in both sets of animals.

Tissue Distribution of (S)-4'-(HO)-DADFT-PE (11). One of the toxicity issues surrounding iron chelation therapy is the problem of renal damage. Many iron chelators have been shown to have untoward effects at the proximal tubule level. This is certainly one of the dose-limiting toxicities of several of the DFT analogues and the Novartis triazole ICL670A. Although a structure–activity study made it possible to largely ameliorate the nephrotoxicity of DFT, as realized in (S)-4'-(HO)-DADFT (**1**), it is not entirely absent at high doses. This observation compelled us to further search for a DFT analogue that would maintain an iron-clearing efficiency similar to **1** but would accumulate to a lesser extent in the kidney. In the current study, we compare the tissue distribution of the polyether **11** and its metabolite **1** with those for **1** itself and (S)-4'-(CH₃O)-DADFT (**6**) and its metabolite **1** (Figure 2). The organs chosen in addition

to the kidneys, e.g., the liver, pancreas, and heart, are the tissues most negatively affected by iron overload.

Each rat was given a single sc 300 μmol/kg dose of the drug, and the animals were sacrificed 2, 4, 6, and 8 h after dosing. In the plasma, although neither **1** nor **11** ever achieved levels above 10 μM, very small amounts of the polyether metabolite **1** were observed. In contrast, **6** rose to levels in the plasma of 470 μM at 2 h, dropping to 75 μM at 8 h. Very little of **1**, the metabolite of **6**, was observed (Figure 2A).

All of the drugs achieved fairly high levels in the liver (Figure 2B). The concentration of the parent drug **1** was 48 ± 20 nmol/g wet weight at 2 h, dropping to 12 ± 0.8 nmol/g wet weight at 8 h. The 4'-(CH₃O) analogue (**6**) and its metabolite (**1**) reached 155 ± 13 nmol/g wet weight 2 h postdrug. The metabolite represents 28% of the total of the components. At 8 h the total drug dropped to 106 ± 19 nmol/g wet weight, 23% of which is the metabolite. The polyether (**11**) and its metabolite (**1**) reached 134 ± 32 nmol/g wet weight at 2 h, 2% as the metabolite. At 8 h the polyether dropped to 25 ± 5 nmol/g wet weight with no measurable metabolite. The liver levels relative to the plasma of ligands **1** and **11** suggest first-pass clearance.

The ligands do not concentrate to a great extent in the pancreas (Figure 2C). At 2 h postdosing **1** has achieved 6 ± 1 nmol/g wet weight and is not detectable at future time points. The polyether (**11**) reaches a concentration of 30 ± 25 nmol/g wet weight at 2 h, dropping to 3 ± 3 nmol/g wet weight at 8 h. The 4'-(CH₃O) ligand (**6**) also rises to 38 ± 5 nmol/g wet weight

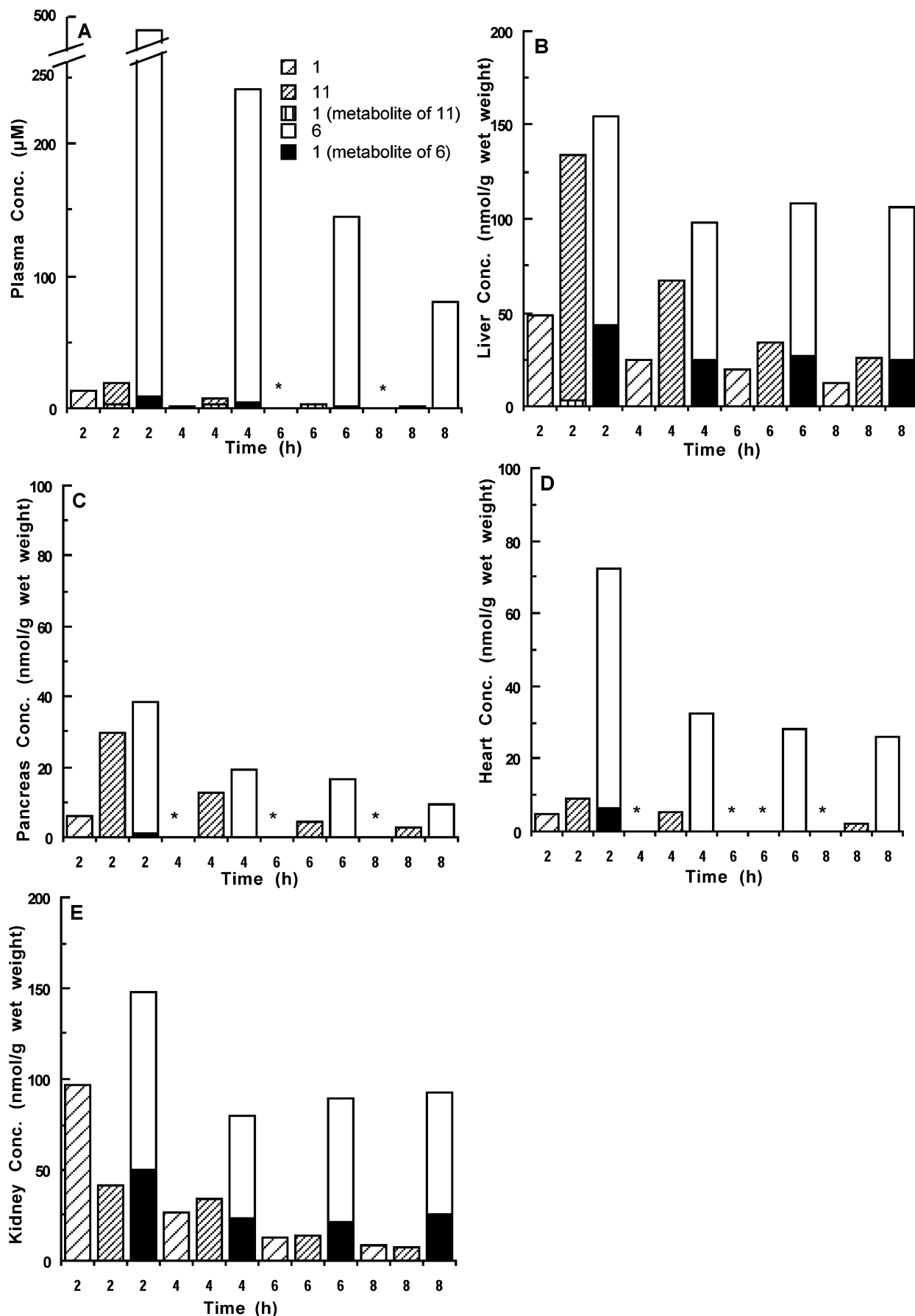


Figure 2. Distribution in plasma (A), liver (B), pancreas (C), heart (D), and kidney (E) of (*S*)-4'-(HO)-DADFT (**1**), (*S*)-4'-(CH₃O)-DADFT (**6**), and (*S*)-4'-(HO)-DADFT-PE (**11**) after a single sc administration. For all time points, $n = 3$. The asterisks indicate a level below detectable limits (ca. 5 nmol/g wet wt). Data for **1** and **6** are from ref 42.

at 2 h, dropping to around 8 nmol/g wet weight at 8 h. A small amount of **1**, the metabolite of **6**, was observed at 2 h.

The drug levels in the heart are very interesting (Figure 2D). The parent drug (**1**) is found only at 2 h postdrug and even then only at 5 ± 3 nmol/g wet weight. Ligand **11** also achieves very low concentrations. At 2 h it is just 9 ± 3 nmol/g wet weight, dropping to 5 ± 1 nmol/g wet weight at 4 h, not detectable at 6 h, and only 2 ± 2 nmol/g wet weight at 8 h. In contrast, **6** and its metabolite (**1**) are present at 73 ± 3 nmol/g wet weight at 2 h; 9% is in the form of the metabolite (**1**). This drops to 33 ± 4 nmol/g wet at 4 h and remains fairly steady through the 8 h time point.

The kidney drug levels are probably most cogent to the current study (Figure 2E). Both the parent ligand (**1**) and its methoxy analogue (**6**) achieve fairly high levels in the kidney. Ligand **1** is nearly 100 nmol/g wet weight at 2 h, dropping to 9 ± 3 nmol/g wet weight at 8 h. Ligand **6** and its metabolite (**1**) reach nearly 150 nmol/g wet weight at 2 h; 34% is in the form of the metabolite. The concentration then remains >80 nmol/g wet weight through 8 h postdrug. However, the renal concentration of polyether (**11**) is only 41 ± 3 nmol/g wet weight at 2 h and decreases to less than 10 nmol/g wet weight at 8 h. These tissue concentrations ($6 > 1 > 11$) seem to be in keeping with the compounds' nephrotoxicity profiles.

A Comparison of the Impact of (S)-4'-(HO)-DADFT-PE (11) and (S)-4'-(HO)-DADFT (1) on Rodent Kidneys. In a preliminary dose-range finding study, male Sprague-Dawley rats were given **1** twice daily for 7 days at doses of 237, 355, or 474 $\mu\text{mol/kg/dose}$ (474, 711, or 947 $\mu\text{mol/kg/d}$). The drug was found to cause moderate to severe vacuolization in the renal proximal tubules at all doses. It was decided that the 237 $\mu\text{mol/kg/dose}$ (474 $\mu\text{mol/kg/d}$) would be used to compare the renal toxicity of **1** with that of the polyether (**11**).

A total of 12 rats were used for this study: four controls, four treated with **11**, and four treated with **1**. The two drugs **11** and **1** were given po by gavage to the rodents twice daily for 7 days at equimolar doses of 237 $\mu\text{mol/kg/dose}$ (474 $\mu\text{mol/kg/d}$). One day postdrug the kidneys were perfusion-fixed and one kidney from each rat was dissected. Tissue samples of 1 mm³ were cut from the kidney cortexes. Under light microscopy the proximal and distal tubules of kidneys from the control animals show normal tubular architecture (Figure 3A). The proximal tubules of kidneys from the polyether (**11**) treated rodents (Figure 3B) are indistinguishable from those of the control animals (Figure 3A); the distal tubules present with occasional vacuolization but are otherwise normal. However, animals treated with **1** (Figure 3C) show regional, moderate to severe vacuolization in the proximal tubules, a loss of the brush border, and tubular extrusions toward the lumen; the distal tubules show moderate to severe vacuolization.

Under electron microscopy the kidneys from the control animals show normal proximal and distal tubular architecture (photographs not shown). Kidneys from animals treated with the polyether (**11**) present with occasional vacuolization and apoptotic nuclei and have some abnormal giant lysosomes at the basolateral side of the proximal tubule but are otherwise normal. The same is true of the distal tubules. Finally, animals treated with **1** show regional, moderate to severe vacuolization of the proximal tubules (mainly S2 segments), loss of the brush border, golgi dilations, tubular extrusions toward the lumen, and apoptotic nuclei. The distal tubules demonstrate moderate to severe vacuolization. While the distal tubules of both the polyether **11** and the parent **1** treated animals do demonstrate some vacuolization, the changes to the kidneys of the animals

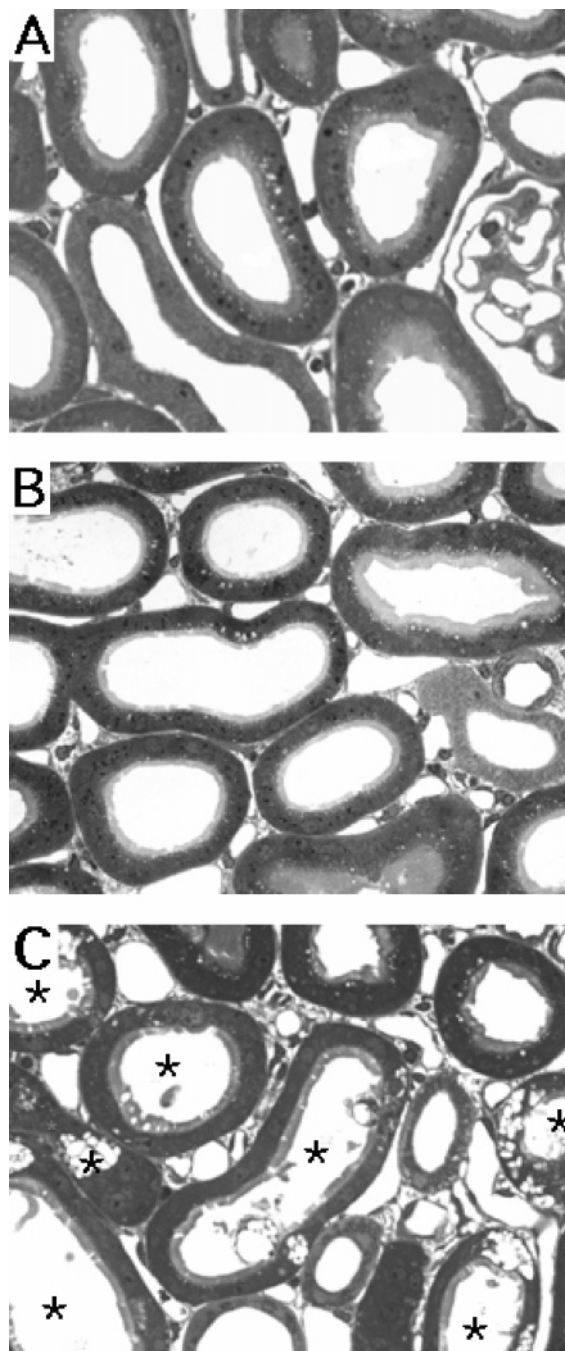


Figure 3. The impact of (S)-4'-(HO)-DADFT-PE (**11**) and (S)-4'-(HO)-DADFT (**1**) on rat kidney proximal tubules as compared with untreated rats (control). The drugs were given po twice daily for 7 days at a dose of 237 $\mu\text{mol/kg/dose}$ (474 $\mu\text{mol/kg/d}$). The proximal tubules from rats treated with **11** (B) are almost indistinguishable from those of the control animals (A). However, the proximal tubules from rats treated with **1** (C) display moderate to severe damage (tubules marked with an asterisk). Magnification = 400 \times .

treated with **1** are much more pronounced. These findings are in keeping with the level of **11** achieved in the kidney relative to that of **1**.

Conclusion

Our previous studies revealed that within a family of ligands the more lipophilic chelators have better iron-clearing efficiency, i.e., the larger the log P_{app} value of the compound, the better the iron-clearing efficiency. What is also clear from the data is that although the relative effects of log P_{app} changes are essentially the same through different families, there are real

differences in absolute value. For example, increasing the lipophilicity of (*S*)-4'-(HO)-DADMDFT (**4**) and (*S*)-3'-(HO)-DADMDFT (**7**) increased the iron-clearing efficiencies about as effectively (Table 1). However, the (*S*)-3'-(HO)-DADFT ligands (**7–10**) were consistently more efficient.⁴²

There also exists a second, albeit somewhat more disturbing, relationship. In all sets of ligands, the more lipophilic chelator is always the more toxic. The current study focuses on designing ligands that balance the lipophilicity/toxicity interaction while iron-clearing efficiency is maintained. Earlier studies with (*S*)-4'-(CH₃O)-DADFT (**6**) indicated that this methyl ether had excellent iron-clearing efficiency in both rodents and primates; however, it was too toxic. This established that the 4'-(HO) functionality of (*S*)-4'-(HO)-DADFT (**1**) was not requisite for iron-clearing function. On the basis of this finding, a less lipophilic, more water-soluble ligand than **6** was assembled, the polyether (*S*)-4'-(HO)-DADFT-PE (**11**), along with its ethyl (**16**) and isopropyl (**15**) esters. The key step in the synthesis of this ligand was the coupling of tri(ethylene glycol) monomethyl ether with isopropyl 2-(2,4-dihydroxyphenyl)-4,5-dihydro-4-methyl-4-thiazolecarboxylate (**14**) under Mitsunobu conditions in the presence of diisopropyl azodicarboxylate and triphenylphosphine.

When **1** was 4'-(HO) methylated to provide **6**, the iron-clearing efficiency after po administration increased substantially to $6.6 \pm 2.8\%$ in a rodent model. The polyether (**11**), in which a 3,6,9-trioxadecyl group was fixed to the 4'-(HO) of **1**, also performed well, with an iron-clearing efficiency of $5.5 \pm 1.9\%$ when administered po. Given sc, the efficiency increased to $8.7 \pm 2.6\%$, slightly more than po ($p < 0.05$). The iron-clearing efficiency of the corresponding isopropyl ester, (*S*)-4'-(HO)-DADFT-PE-*i*PrE (**15**), was significantly higher than the polyether parent **11** when administered po, $13.9 \pm 3.3\%$ versus $5.5 \pm 1.9\%$ ($p < 0.002$). When administered sc, the isopropyl ester (**15**) was also significantly better than **11**, $22.1 \pm 7.6\%$ versus $8.7 \pm 2.6\%$ ($p < 0.003$). Although the isopropyl ester (**15**) is only a bidentate ligand, nonspecific esterase cleavage would liberate the tridentate chelator, **11**.

The efficiency of the 4'-(CH₃O) analogue (**6**) given po to primates was $24.4 \pm 10.8\%$. The corresponding polyether (**11**) given po performed very well in primates, with an efficiency of $25.4 \pm 7.4\%$. When given sc the efficiency was $30.4 \pm 7.2\%$, not significantly better than when given po.

In addition, both the parent ligand (**1**) and the polyether analogue (**11**) demonstrate excellent oral bioavailability in the iron-loaded primates. The po vs sc iron clearing efficiencies are nearly identical: $16.8 \pm 7.2\%$ vs $15.9 \pm 2.7\%$ for ligand **1** and $25.4 \pm 7.4\%$ vs $30.4 \pm 7.2\%$ for **11**. The po and sc iron clearing efficiencies of **11** are 500% greater than that of sc administered DFO.³⁸

A comparison of **11** in rodents with **1** revealed the polyether to be more tolerable, achieving higher concentrations in the liver and significantly lower concentrations in the kidney. The kidney drug levels are probably most cogent to the current study. Both the parent ligand (*S*)-4'-(HO)-DADFT (**1**) and its methoxy analogue **6** achieve fairly high levels in the kidney. Ligand **1** is nearly 100 nmol/g wet weight at 2 h, dropping to 9 ± 3 nmol/g wet weight at 8 h. Ligand **6** and its metabolite **1** reach nearly 150 nmol/g wet weight at 2 h; 34% is in the form of the metabolite. The concentration then remains >80 nmol/g wet weight through 8 h postdrug. However, the polyether (**11**) renal concentration is only 41 ± 3 nmol/g wet weight at 2 h and decreases to less than 10 nmol/g wet weight at 8 h. These tissue concentrations ($6 > 1 > 11$) seem to be in keeping with the

compounds' nephrotoxicity profiles. The lower renal concentrations of **11** relative to **1** are in keeping with the profound difference in architectural changes seen in the kidneys of rodents given each drug.

Under light microscopy, the proximal and distal tubules of kidneys from the control animals show normal tubular architecture. The proximal tubules of kidneys from the polyether (**11**) treated rodents are indistinguishable from those of the control animals; the distal tubules present with occasional vacuolization but are otherwise normal. However, animals treated with **1** show regional, moderate to severe vacuolization in the proximal tubules, a loss of the brush border, and tubular extrusions toward the lumen; the distal tubules show moderate to severe vacuolization.

Under electron microscopy the kidneys from the control animals show normal proximal and distal tubular architecture. Kidneys from animals treated with the polyether (**11**) present with occasional vacuolization and apoptotic nuclei and have some abnormal giant lysosomes at the basolateral side of the proximal tubule but are otherwise normal. The same is true of the distal tubules. Finally, animals treated with **1** show regional, moderate to severe vacuolization of the proximal tubules (mainly S2 segments), loss of the brush border, golgi dilations, tubular extrusions toward the lumen, and apoptotic nuclei. The distal tubules demonstrate moderate to severe vacuolization. While the distal tubules of both the polyether **11** and the parent **1** treated animals do demonstrate some vacuolization, the changes to the kidneys of the animals treated with **1** are much more pronounced. These findings are in keeping with the level of **11** achieved in the kidney relative to that of **1**.

These data are consistent with the idea that further preclinical studies of **11** are warranted, particularly longer-term toxicity studies and pharmacokinetics.

Experimental Section

C. apella monkeys were obtained from World Wide Primates (Miami, FL). Male Sprague–Dawley rats were procured from Harlan Sprague–Dawley (Indianapolis, IN). Cremophor RH-40 was obtained from BASF (Parsippany, NJ). Ultrapure salts were obtained from Johnson Matthey Electronics (Royston, UK). All hematological and biochemical studies³⁸ were performed by Antech Diagnostics (Tampa, FL). Atomic absorption (AA) measurements were made on a Perkin-Elmer model 5100 PC (Norwalk, CT). Histopathological analysis was carried out by Florida Vet Path (Bushnell, FL).

Cannulation of Bile Duct in Non-Iron-Overloaded Rats. The cannulation has been described previously.^{37,38} Bile samples were collected from male Sprague–Dawley rats (400–450 g) at 3-h intervals for 24 h. The urine sample was taken at 24 h. Sample collection and handling are as previously described.^{37,38}

Iron Loading of *C. apella* Monkeys. The monkeys (3.5–4 kg) were iron overloaded with iv iron dextran as specified in earlier publications to provide about 500 mg of iron per kg of body weight;⁴³ the serum transferrin iron saturation rose to between 70 and 80%. At least 20 half-lives, 60 d,⁴⁴ elapsed before any of the animals were used in experiments evaluating iron-chelating agents.

Primate Fecal and Urine Samples. Fecal and urine samples were collected at 24-h intervals and processed as described previously.^{37,38,45} Briefly, the collections began 4 d prior to the administration of the test drug and continued for an additional 5 d after the drug was given. Iron concentrations were determined by flame atomic absorption spectroscopy as presented in other publications.^{37,46}

Drug Preparation and Administration. In the iron-clearing experiments the rats were given a single 300 μ mol/kg dose of the drugs po and/or sc. The compounds were administered as (1) a solution in water (**11**); (2) solubilized in 40% Cremophor RH-40/

water (**15**, po); (3) the monosodium salt of the compound of interest (prepared by addition of the free acid to 1 equivalent of NaOH) (**1**, **6**); or (4) in 50% ethanol–water (**15** sc and **16**). Cremophor was utilized as the vehicle for the po (but not sc) dosing of **15** because of the potential for 50% aqueous ethanol to cause gastric ulceration that could lead to increased drug absorption and falsely increased iron clearance.

The drugs were given to the monkeys po and/or sc at a dose of 150 $\mu\text{mol/kg}$. The drugs were prepared as for the rats, except that **6** was solubilized in 40% Cremophor RH-40/water.

Calculation of Iron Chelator Efficiency. The theoretical iron outputs of the chelators were generated on the basis of a 2:1 complex. The efficiencies in the rats and monkeys were calculated as set forth elsewhere.⁴⁰ Data are presented as the mean \pm the standard error of the mean; *P*-values were generated via a one-tailed Student's *t*-test, in which the inequality of variances was assumed; and a *P*-value of <0.05 was considered significant.

Toxicity Evaluation of (S)-4'-CH₃O-DADFT (6**) and the Polyether Acid (**11**) in Rodents.** Male Sprague–Dawley rats (250–300 g) were fasted overnight and were given **6** or **11** po by gavage once daily for up to 10 d at a dose of 384 $\mu\text{mol/kg/d}$. This dose is equivalent to 100 mg/kg/d of the DFT sodium salt. The animals were fed ~ 3 h postdrug and had access to food for 5 h before being fasted overnight. The rats given **11** in the 30-day experiment were given the drug po at a dose of 63.3 $\mu\text{mol/kg/d}$, a dose that, in the primates, results in the excretion of 450 μg of Fe/kg. Due to the protracted nature of the latter experiment, the animals were not fasted. To minimize food content in the stomach, the drug was not given until the afternoon. Additional animals served as age-matched controls.

Collection of Tissue Samples from Rodents. Male Sprague–Dawley rats (250–350 g) were given a single sc injection of **1**, **6**, and **11** at a dose of 300 $\mu\text{mol/kg}$ prepared as described above. At times 2, 4, 6, and 8 h after dosing ($n = 3$ rats per time point) the animals were euthanized by exposure to CO₂ gas. Blood was obtained via cardiac puncture into vacutainers containing sodium citrate. The blood was centrifuged and the plasma separated for analysis. The liver, heart, kidneys, and pancreas were then removed from the animals.

Tissue Analytical Methods. The tissue samples were prepared for HPLC analysis by homogenizing them in water at a ratio of 1:2 (w/v). Then, to precipitate proteins, three times the volume of CH₃OH was added, and the mixture was stored at -20 °C for 20 min. This homogenate was centrifuged; the supernatant was filtered with a 0.2 μm membrane. The filtrate was injected directly onto the column or diluted with mobile phase A (95% buffer [25 mM KH₂PO₄, pH 3.0]:5% CH₃CN), vortexed, and filtered as above prior to injection.

Analytical separation was performed on a Discovery RP Amide C₁₆ HPLC system with UV detection at 310 nm as described previously.^{47,48} Mobile phase and chromatographic conditions were as follows: solvent A, 5% CH₃CN:95% buffer; solvent B, 60% CH₃CN:40% buffer. The gradients for compounds **1**, **6**, and **11** were a linear ramp from 100% A to 50% A (9 min), followed by a hold of 10 min.

The concentrations were calculated from the peak area fitted to calibration curves by nonweighted least squares linear regression with Rainin Dynamax HPLC Method Manager software (Rainin Instrument Co.). The method had a detection limit of 0.5 μM and was reproducible and linear over a range of 1–1000 μM .

A Comparison of the Impact of (S)-4'-(HO)-DADFT-PE (11**) and (S)-4'-(HO)-DADFT (**1**) on Rodent Kidneys.** Male Sprague–Dawley rats (200–250 g) were housed two to a cage and were fasted overnight. The rats were given **11** or **1** po twice daily at a dose of 237 $\mu\text{mol/kg/dose}$ (474 $\mu\text{mol/kg/d}$) for 7 days. The rats were fed approximately 3 h postdrug and had access to food for 5 h before being fasted again.

One day postdrug, the rats were anesthetized with sodium pentobarbital. The abdominal aorta was isolated and cleansed of extraneous tissue and cannulated. The kidneys were perfusion-fixed with glutaraldehyde in Tyrode's buffer containing 3% PVP,

removed, and immersed in a glass vial containing fresh fixative at room temperature. Four hours later, the kidneys were again rinsed with Tyrode's buffer. The tissue samples were placed in sodium cacodylate. After two rinses with cacodylate buffer, the samples were dehydrated with graded concentrations of ethyl alcohol and infiltrated with propylene oxide overnight. Finally, they were embedded in TAAB with DMP-30. The TAAB was polymerized at 60 °C for 48 h.

Thick sections (500 nm) were cut from TAAB embedded tissue, mounted onto glass slides and stained with Toluidine Blue. The tissue slices were photographed with a Zeiss Axioskop II at 400 \times magnification.

For further demonstration of architectural differences, thin slices (50–90 nm) were mounted onto copper grids, stained with uranyl acetate, counterstained with lead nitrate, and evaluated via a Zeiss transmission electron microscope.

Synthetic Methods. Compound **1** was synthesized using the method published by this laboratory.⁴⁰ Reagents were purchased from Aldrich Chemical Co. (Milwaukee, WI), and Fisher Optima-grade solvents were routinely used. DMF and THF were distilled, the latter from sodium and benzophenone. Reactions were run under a nitrogen atmosphere, and organic extracts were dried with sodium sulfate. Silica gel 40–63 from SiliCycle, Inc. (Quebec City, QC, Canada) was used for flash column chromatography. Optical rotations were run at 589 nm (sodium D line) utilizing a Perkin-Elmer 341 polarimeter, with *c* being concentration in grams of compound per 100 mL of CHCl₃ solution. Chemical shifts (δ) for ¹H NMR spectra are given in parts per million downfield from tetramethylsilane for CDCl₃ (not indicated) or sodium 3-(trimethylsilyl)propionate-2,2,3,3-*d*₄ for D₂O. NOE difference spectra at 500 and 750 MHz were obtained as follows: specified resonances of non-degassed samples in CDCl₃ were irradiated for 2.5–3.0 s prior to acquisition of the spectra with saturation, and from these were subtracted control spectra with irradiation off resonance. Chemical shifts (δ) for ¹³C NMR spectra are given in parts per million referenced to 1,4-dioxane (δ 67.19) in D₂O or to the residual solvent resonance in CDCl₃ (δ 77.16). Coupling constants (*J*) are in hertz. Elemental analyses were performed by Atlantic Microlabs (Norcross, GA).

Isopropyl 2-(2,4-Dihydroxyphenyl)-4,5-dihydro-4-methyl-4-thiazolecarboxylate (14**).** 2-Iodopropane (4.0 mL, 40 mmol) and DIEA (7.0 mL, 40 mmol) were successively added to **1** (5.32 g, 21.0 mmol) in DMF (65 mL), and the solution was stirred at room temperature for 14 d. After solvent removal under high vacuum, the residue was treated with 1:1 0.5 M citric acid/saturated NaCl (200 mL) and was extracted with EtOAc (200 mL, 2 \times 50 mL). The combined extracts were washed with 100-mL portions of 0.25 M citric acid, 1% NaHSO₃, H₂O, and saturated NaCl, and solvent was evaporated. Purification by flash column chromatography using 20% EtOAc/toluene furnished 6.1 g (99%) of **14** as a yellow oil: [α]_D²⁶ +64.3° (*c* 1.00); 300 MHz ¹H NMR δ 1.27 and 1.29 (2 d, 6 H, *J* = 5.5), 1.64 (s, 3 H), 3.18 (d, 1 H, *J* = 11.3), 3.82 (d, 1 H, *J* = 11.2), 5.08 (septet, 1 H, *J* = 6.3), 6.37 (dd, 1 H, *J* = 8.5, 2.5), 6.43 (d, 1 H, *J* = 2.4), 7.27 (d, 1 H, *J* = 8.5) 12.8 (br s, 1 H); 125.8 MHz ¹³C NMR δ 21.70, 24.46, 39.86, 69.89, 83.18, 103.20, 107.58, 109.97, 132.24, 160.79, 161.28, 171.03, 172.75. Anal. (C₁₄H₁₇NO₄S) C, H, N.

Isopropyl (S)-4,5-Dihydro-2-[2-hydroxy-4-(3,6,9-trioxadecyloxy)phenyl]-4-methyl-4-thiazolecarboxylate (15**).** Tri(ethylene glycol) monomethyl ether (1.6 mL, 10 mmol) and diisopropyl azodicarboxylate (2.3 mL, 12 mmol) were successively added to a solution of **14** (2.89 g, 9.78 mmol) and triphenylphosphine (3.07 g, 11.7 mmol) in THF (60 mL) with ice bath cooling. The solution was stirred at room temperature for 3 h and was maintained at 5 °C for 16 h. Solvent was removed by rotary evaporation, and 40% EtOAc/petroleum ether (40 mL) was added. The solution was kept at 5 °C for 12 h; solid formed and was filtered and washed with solvent (90 mL). The filtrate was concentrated in vacuo and was purified by flash chromatography (48% EtOAc/petroleum ether) to give 3.29 g of **15** (76%) as a yellow oil: [α]_D²⁶ +40.6° (*c* 1.16); 750 MHz ¹H NMR δ , see Figure 1; 188.6 MHz ¹³C NMR δ 21.76,

24.51, 39.89, 59.19, 67.71, 69.61, 69.66, 70.75, 70.82, 71.04, 72.10, 83.36, 101.60, 107.41, 110.09, 131.78, 161.35, 163.12, 170.75, 172.39. Anal. (C₂₁H₃₁NO₇S) C, H, N.

(S)-4,5-Dihydro-2-[2-hydroxy-4-(3,6,9-trioxadecyloxy)phenyl]-4-methyl-4-thiazolecarboxylic Acid (11). A solution of 50% (w/w) NaOH (4.9 mL, 94 mmol) in CH₃OH (50 mL) was added to **15** (3.24 g, 7.34 mmol) in CH₃OH (100 mL) with ice bath cooling. The reaction mixture was stirred at room temperature for 17 h, and the bulk of the solvent was removed by rotary evaporation. The residue was treated with dilute NaCl (150 mL) and was extracted with ether (3 × 50 mL). The basic aqueous phase was cooled in ice, acidified with 1 N HCl (120 mL), and extracted with EtOAc (200 mL, 2 × 100 mL). After the EtOAc layers were washed with saturated NaCl (100 mL), glassware that was presoaked in 3 N HCl for 15 min was employed henceforth. After solvent removal by rotary evaporation, the residue was dissolved in distilled H₂O (70 mL) and lyophilized to furnish 2.78 g of **11** (95%) as an orange oil: [α]_D²⁵ +53.1° (c 0.98); 400 MHz ¹H NMR (D₂O) δ 1.76 (s, 3 H), 3.35 (s, 3 H), 3.54–3.61 (m, 3 H), 3.64–3.72 (m, 4 H), 3.74–3.78 (m, 2 H), 3.90–3.94 (m, 2 H), 3.96 (d, 1 H, *J* = 12.0), 4.25–4.29 (m, 2 H), 6.53 (d, 1 H, *J* = 2.4), 6.64 (dd, 1 H, *J* = 9.0, 2.2), 7.61 (d, 1 H, *J* = 9.2); 100 MHz ¹³C NMR (D₂O) δ 23.65, 39.56, 58.65, 68.34, 69.33, 70.07, 70.18, 70.44, 71.62, 77.58, 102.11, 106.72, 109.66, 134.67, 161.27, 167.07, 176.86, 180.70. Anal. (C₁₈H₂₅NO₇S) C, H, N.

Ethyl (S)-4,5-Dihydro-2-[2-hydroxy-4-(3,6,9-trioxadecyloxy)phenyl]-4-methyl-4-thiazolecarboxylate (16). Iodoethane (0.25 mL, 3.1 mmol) and DIEA (0.55 mL, 3.2 mmol) were successively added to **11** (0.781 g, 1.95 mmol) in DMF (31 mL), and the solution was stirred at room temperature for 50 h. After solvent removal under high vacuum, the residue was treated with 1:1 0.5 M citric acid/saturated NaCl (85 mL) and was extracted with EtOAc (4 × 60 mL). The combined extracts were washed with 50-mL portions of 1% NaHSO₃, H₂O, and saturated NaCl, and solvent was evaporated. Purification by flash column chromatography using 1.5:2.5:6 EtOAc/petroleum ether/CH₂Cl₂ furnished 0.690 g (83%) of **16** as an oil: [α]_D²³ +40.2 (c 1.09); 400 MHz ¹H NMR δ 1.30 (t, 3 H, *J* = 7.2) 1.66 (s, 3 H), 3.19 (d, 1 H, *J* = 11.2), 3.38 (s, 3 H), 3.54–3.57 (m, 2 H), 3.64–3.70 (m, 4 H), 3.72–3.76 (m, 2 H), 3.81–3.88 (m, 3 H), 4.12–4.17 (m, 2 H), 4.20–4.28 (m, 2 H), 6.46 (dd, 1 H, *J* = 8.8, 2.4), 6.49 (d, 1 H, *J* = 2.4), 7.28 (d, 1 H, *J* = 8.4), 12.69 (s, 1 H). Anal. (C₂₀H₂₉NO₇S) C, H, N.

Acknowledgment. Funding was provided by the National Institutes of Health Grant No. RO1-DK49108. We thank Elizabeth M. Nelson and Katie Ratliff-Thompson for their technical assistance and Carrie A. Blaustein for her editorial and organizational support.

Supporting Information Available: Elemental analytical data for synthesized compounds. This material is available free of charge via the Internet at <http://pubs.acs.org>.

References

- Ponka, P. Physiology and Pathophysiology of Iron Metabolism: Implications for Iron Chelation Therapy in Iron Overload. In *The Development of Iron Chelators for Clinical Use*; Bergeron, R. J., Brittenham, G. M., Eds.; CRC: Boca Raton, FL, 1994; pp 1–29.
- Olivieri, N. F.; Brittenham, G. M. Iron-chelating Therapy and the Treatment of Thalassemia. *Blood* **1997**, *89*, 739–761.
- Vichinsky, E. P. Current Issues with Blood Transfusions in Sickle Cell Disease. *Semin. Hematol.* **2001**, *38*, 14–22.
- Kersten, M. J.; Lange, R.; Smeets, M. E.; Vreugdenhil, G.; Roozendaal, K. J.; Lameijer, W.; Goudsmit, R. Long-Term Treatment of Transfusional Iron Overload with the Oral Iron Chelator Deferiprone (L1): A Dutch Multicenter Trial. *Ann. Hematol.* **1996**, *73*, 247–252.
- Conrad, M. E.; Umbreit, J. N.; Moore, E. G. Iron Absorption and Transport. *Am. J. Med. Sci.* **1999**, *318*, 213–229.
- Lieu, P. T.; Heiskala, M.; Peterson, P. A.; Yang, Y. The Roles of Iron in Health and Disease. *Mol. Aspects Med.* **2001**, *22*, 1–87.
- Angelucci, E.; Brittenham, G. M.; McLaren, C. E.; Ripalti, M.; Baronciani, D.; Giardini, C.; Galimberti, M.; Polchi, P.; Lucarelli, G. Hepatic Iron Concentration and Total Body Iron Stores in Thalassemia Major. *N. Engl. J. Med.* **2000**, *343*, 327–331.
- Bonkovsky, H. L.; Lambrecht, R. W. Iron-Induced Liver Injury. *Clin. Liver Dis.* **2000**, *4*, 409–429, vi–vii.
- Pietrangelo, A. Mechanism of Iron Toxicity. *Adv. Exp. Med. Biol.* **2002**, *509*, 19–43.
- Cario, H.; Holl, R. W.; Debatin, K. M.; Kohne, E. Insulin Sensitivity and β-Cell Secretion in Thalassemia Major with Secondary Haemochromatosis: Assessment by Oral Glucose Tolerance Test. *Eur. J. Pediatr.* **2003**, *162*, 139–146.
- Wojcik, J. P.; Speechley, M. R.; Kertesz, A. E.; Chakrabarti, S.; Adams, P. C. Natural History of C282Y Homozygotes for Hemochromatosis. *Can. J. Gastroenterol.* **2002**, *16*, 297–302.
- Brittenham, G. M.; Griffith, P. M.; Nienhuis, A. W.; McLaren, C. E.; Young, N. S.; Tucker, E. E.; Allen, C. J.; Farrell, D. E.; Harris, J. W. Efficacy of Deferoxamine in Preventing Complications of Iron Overload in Patients with Thalassemia Major. *N. Engl. J. Med.* **1994**, *331*, 567–573.
- Brittenham, G. M. Disorders of Iron Metabolism: Iron Deficiency and Overload. In *Hematology: Basic Principles and Practice*, 3rd ed.; Hoffman, R., Benz, E. J., Shattil, S. J., Furie, B., Cohen, H. J., et al., Eds.; Churchill Livingstone: New York, 2000; pp 397–428.
- Zurlo, M. G.; De Stefano, P.; Borgna-Pignatti, C.; Di Palma, A.; Piga, A.; Melevendi, C.; Di Gregorio, F.; Burattini, M. G.; Terzoli, S. Survival and Causes of Death in Thalassemia Major. *Lancet* **1989**, *2*, 27–30.
- Oudit, G. Y.; Sun, H.; Trivieri, M. G.; Koch, S. E.; Dawood, F.; Ackerley, C.; Yazdanpanah, M.; Wilson, G. J.; Schwartz, A.; Liu, P. P.; Backx, P. H. L-type Ca²⁺ Channels Provide a Major Pathway for Iron Entry into Cardiomyocytes in Iron-Overload Cardiomyopathy. *Nat. Med.* **2003**, *9*, 1187–1194.
- Graf, E.; Mahoney, J. R.; Bryant, R. G.; Eaton, J. W. Iron-Catalyzed Hydroxyl Radical Formation. Stringent Requirement for Free Iron Coordination Site. *J. Biol. Chem.* **1984**, *259*, 3620–3624.
- Halliwell, B. Free Radicals and Antioxidants: A Personal View. *Nutr. Rev.* **1994**, *52*, 253–265.
- Halliwell, B. Iron, Oxidative Damage, and Chelating Agents. In *The Development of Iron Chelators for Clinical Use*; Bergeron, R. J., Brittenham, G. M., Eds.; CRC: Boca Raton, FL, 1994; pp 33–56.
- Koppenol, W. Kinetics and Mechanism of the Fenton Reaction: Implications for Iron Toxicity. In *Iron Chelators: New Development Strategies*; Badman, D. G., Bergeron, R. J., Brittenham, G. M., Eds.; Saratoga: Ponte Vedra Beach, FL, 2000; pp 3–10.
- Dean, R. T.; Nicholson, P. The Action of Nine Chelators on Iron-Dependent Radical Damage. *Free Radic. Res.* **1994**, *20*, 83–101.
- Porter, J. B. Deferoxamine Pharmacokinetics. *Semin. Hematol.* **2001**, *38*, 63–68.
- Lee, P.; Mohammed, N.; Marshall, L.; Abeyinghe, R. D.; Hider, R. C.; Porter, J. B.; Singh, S. Intravenous Infusion Pharmacokinetics of Desferrioxamine in Thalassemic Patients. *Drug Metab. Dispos.* **1993**, *21*, 640–644.
- Pippard, M. J.; Callender, S. T.; Finch, C. A. Ferrioxamine Excretion in Iron-Loaded Man. *Blood* **1982**, *60*, 288–294.
- Pippard, M. J. Desferrioxamine-Induced Iron Excretion in Humans. *Bailliere's Clin. Haematol.* **1989**, *2*, 323–343.
- Hoffbrand, A. V.; Al-Rafaie, F.; Davis, B.; Siritanakatkul, N.; Jackson, B. F. A.; Cochrane, J.; Prescott, E.; Wonke, B. Long-term Trial of Deferiprone in 51 Transfusion-Dependent Iron Overloaded Patients. *Blood* **1998**, *91*, 295–300.
- Olivieri, N. F. Long-term Therapy with Deferiprone. *Acta Haematol.* **1996**, *95*, 37–48.
- Olivieri, N. F.; Brittenham, G. M.; McLaren, C. E.; Templeton, D. M.; Cameron, R. G.; McClelland, R. A.; Burt, A. D.; Fleming, K. A. Long-Term Safety and Effectiveness of Iron-Chelation Therapy with Deferiprone for Thalassemia Major. *N. Engl. J. Med.* **1998**, *339*, 417–423.
- Richardson, D. R. The Controversial Role of Deferiprone in the Treatment of Thalassemia. *J. Lab. Clin. Med.* **2001**, *137*, 324–329.
- Nisbet-Brown, E.; Olivieri, N. F.; Giardina, P. J.; Grady, R. W.; Neufeld, E. J.; Sechard, R.; Krebs-Brown, A. J.; Anderson, J. R.; Alberti, D.; Sizer, K. C.; Nathan, D. G. Effectiveness and Safety of ICL670 in Iron-Loaded Patients with Thalassemia: A Randomised, Double-Blind, Placebo-Controlled, Dose-Escalation Trial. *Lancet* **2003**, *361*, 1597–1602.
- Galanello, R.; Piga, A.; Alberti, D.; Rouan, M.-C.; Bigler, H.; Séchard, R. Safety, Tolerability, and Pharmacokinetics of ICL670, a New Orally Active Iron-Chelating Agent in Patients with Transfusion-Dependent Iron Overload Due to β-Thalassemia. *J. Clin. Pharmacol.* **2003**, *43*, 565–572.
- Capellini, M. D. Iron-Chelating Therapy with the New Oral Agent ICL670 (Exjade). *Best Pract. Res. Clin. Haematol.* **2005**, *18*, 289–298.
- Davis, B. A.; Porter, J. B. Long-Term Outcome of Continuous 24-Hour Deferoxamine Infusion via Indwelling Intravenous Catheters in High-Risk β-Thalassemia. *Blood* **2000**, *95*, 1229–1236.

- (33) Naegeli, H.-U.; Zähler, H. Metabolites of Microorganisms. Part 193. Ferrithiocin. *Helv. Chim. Acta* **1980**, *63*, 1400–1406.
- (34) Hahn, F. E.; McMurry, T. J.; Hugi, A.; Raymond, K. N. Coordination Chemistry of Microbial Iron Transport. 42. Structural and Spectroscopic Characterization of Diastereomeric Cr(III) and Co(III) Complexes of Desferriferrithiocin. *J. Am. Chem. Soc.* **1990**, *112*, 1854–1860.
- (35) Anderegg, G.; Räber, M. Metal Complex Formation of a New Siderophore Desferrithiocin and of Three Related Ligands. *J. Chem. Soc. Chem. Commun.* **1990**, 1194–1196.
- (36) Bergeron, R. J.; Wiegand, J.; Dionis, J. B.; Egli-Karmakka, M.; Frei, J.; Huxley-Tencer, A.; Peter, H. H. Evaluation of Desferrithiocin and Its Synthetic Analogues as Orally Effective Iron Chelators. *J. Med. Chem.* **1991**, *34*, 2072–2078.
- (37) Bergeron, R. J.; Streiff, R. R.; Wiegand, J.; Vinson, J. R. T.; Luchetta, G.; Evans, K. M.; Peter, H.; Jenny, H.-B. A Comparative Evaluation of Iron Clearance Models. *Ann. N. Y. Acad. Sci.* **1990**, *612*, 378–393.
- (38) Bergeron, R. J.; Streiff, R. R.; Creary, E. A.; Daniels, R. D., Jr.; King, W.; Luchetta, G.; Wiegand, J.; Moerker, T.; Peter, H. H. A Comparative Study of the Iron-Clearing Properties of Desferrithiocin Analogues with Desferrioxamine B in a *Cebus* Monkey Model. *Blood* **1993**, *81*, 2166–2173.
- (39) Bergeron, R. J.; Wiegand, J.; Weimar, W. R.; Vinson, J. R. T.; Bussenius, J.; Yao, G. W.; McManis, J. S. Desazadesmethyl-desferrithiocin Analogues as Orally Effective Iron Chelators. *J. Med. Chem.* **1999**, *42*, 95–108.
- (40) Bergeron, R. J.; Wiegand, J.; McManis, J. S.; McCosar, B. H.; Weimar, W. R.; Brittenham, G. M.; Smith, R. E. Effects of C-4 Stereochemistry and C-4' Hydroxylation on the Iron Clearing Efficiency and Toxicity of Desferrithiocin Analogues. *J. Med. Chem.* **1999**, *42*, 2432–2440.
- (41) Bergeron, R. J.; Wiegand, J.; McManis, J. S.; Bussenius, J.; Smith, R. E.; Weimar, W. R. Methoxylation of Desazadesferrithiocin Analogues: Enhanced Iron Clearing Efficiency. *J. Med. Chem.* **2003**, *46*, 1470–1477.
- (42) Bergeron, R. J.; Wiegand, J.; McManis, J. S.; Weimar, W. R.; Park, J.-H.; Eiler-McManis, E.; Bergeron, J.; Brittenham, G. M. Partition-Variant Desferrithiocin Analogues: Organ Targeting and Increased Iron Clearance. *J. Med. Chem.* **2005**, *48*, 821–831.
- (43) Bergeron, R. J.; Streiff, R. R.; Wiegand, J.; Luchetta, G.; Creary, E. A.; Peter, H. H. A Comparison of the Iron-Clearing Properties of 1,2-Dimethyl-3-hydroxypyrid-4-one, 1,2-Diethyl-3-hydroxypyrid-4-one, and Deferoxamine. *Blood* **1992**, *79*, 1882–1890.
- (44) Wood, J. K.; Milner, P. F.; Pathak, U. N. The Metabolism of Iron-dextran Given as a Total-dose Infusion to Iron Deficient Jamaican Subjects. *Br. J. Haematol.* **1968**, *14*, 119–129.
- (45) Bergeron, R. J.; Wiegand, J.; Brittenham, G. M. HBED: A Potential Alternative to Deferoxamine for Iron-Chelating Therapy. *Blood* **1998**, *91*, 1446–1452.
- (46) Bergeron, R. J.; Wiegand, J.; Wollenweber, M.; McManis, J. S.; Algee, S. E.; Ratliff-Thompson, K. Synthesis and Biological Evaluation of Naphthyl-desferrithiocin Iron Chelators. *J. Med. Chem.* **1996**, *39*, 1575–1581.
- (47) Bergeron, R. J.; Wiegand, J.; Weimar, W. R.; McManis, J. S.; Smith, R. E.; Abboud, K. A. Iron Chelation Promoted by Desazadesferrithiocin Analogues: An Enantioselective Barrier. *Chirality* **2003**, *15*, 593–599.
- (48) Bergeron, R. J.; Wiegand, J.; Ratliff-Thompson, K.; Weimar, W. R. The Origin of the Differences in (*R*)- and (*S*)-Desmethyl-desferrithiocin: Iron-Clearing Properties. *Ann. N.Y. Acad. Sci.* **1998**, *850*, 202–216.

JM0508944